RSC Advances

PAPER

View Article Online
View Journal | View Issue

Cite this: *RSC Adv.*, 2021, **11**, 27085

Neuroinflammatory inhibitors from *Gardneria nutans* Siebold & Zuccarini†

Ying-Ying Si,[ab] Wei-Wei Wang,[a] Qing-Mei Feng,[a] Zhen-Zhu Zhao,[ab] Gui-Min Xue,[ab] Yan-Jun Sun,[ab] Wei-Sheng Feng,[ab] Jun-Im Young*[c] and Xian-Shi Wang*[acd]

Received 6th July 2021
Accepted 3rd August 2021

DOI: 10.1039/d1ra05204g

rsc.li/rsc-advances

Two new monoterpene indole alkaloid glycosides nutanoside A–B (**1–2**), two new phenolic glycoside esters nutanester A–B (**6–7**), together with five known compounds (**3–5**, **8–9**) were isolated from the ethanol extract of *Gardneria nutans* Siebold & Zuccarini. Their structures were established on the basis of extensive spectroscopic analysis and TDDFT/ECD calculations. Compounds **1** and **2** are two rare monoterpene indole alkaloids with the glucosyl moiety located at C-12 and represent the first two examples of enantiomer of ajmaline type monoterpene indole alkaloids. Compounds **3**, **4** and **6** displayed significant inhibitory effects on NO production in over-activated BV2 microglial cells, with the IC_{50} values of 2.29, 6.36, and 8.78 μM, respectively. Compounds **1**, **5**, **7** could significantly inhibit the mRNA expression of inflammatory factors TNF-α and IL-6 induced by LPS in BV2 microglial cells at the effective concentration. Moreover, compound **3** exhibited stronger cytotoxicities against U87 and HCT116 cell lines than taxol with IC_{50} values of 10.58 and 14.60 μM, respectively.

Introduction

Neuroinflammation is considered to be one of the main causes of neurodegenerative diseases like Alzheimer's disease (AD) and Parkinson's disease (PD),[1,2] and microglia cells play an important role in the occurrence and development of neuroinflammation.[3] Microglia cells are the permanent immune cells of central nervous system, which have endogenous immune defense function.[4] Under normal physiological conditions, microglia cells are in a resting or dormant state and provide nutritional support for neurons. In the brain of AD patients, microglia cells can be activated by Aβ and then clear them, thus playing a role in the repair and protection of nervous system.[5] However, over-activation of microglia cells leads to the release of large amounts of inflammatory factors, including nitric oxide (NO), tumor necrosis factor (TNF-α), interleukin (IL-6, IL-1β), reactive oxygen species (ROS) and so on. The continuous and a mass of release of these neurotoxic factors will directly damage neurons, or further activate microglia cells to form a vicious cycle, and eventually lead to the gradual degenerative changes or apoptosis of neurons and the occurrence of neurodegenerative diseases such as AD.[6,7] Therefore, inhibition of over-activation of microglia cells has become an effective way to inhibit neuroinflammation. The lack of effective drugs to treat neuroinflammation has led researchers to turn their attention to natural products.

In our screening of natural herbals for therapy of neuroinflammation, the ethanol extract of *Gardneria nutans* Siebold & Zuccarini was selected as a good candidate. *G. nutans* is derived from the genus *Gardneria* in the Loganiaceae family. The genus *Gardneria* is endemic to Asia and mainly distributed in the southeast of Asia. The plants of this genus are usually used as folk medicines in China, such as *G. multiflora* and *G. angustifolia*.[8,9] Studies on the chemical constituents and pharmacological activities of this genus have revealed that monoterpene indole alkaloids were responsible for diverse bioactivities exhibited by plants of the *Gardneria* genus, including antitumor, sympathetic block, central nervous excitation, dilate blood vessels, reduce blood pressure and nerve conduction[10–14] activities and so on. *G. nutans* is a member of the genus, but there are few reports on its chemical constituents and biological activities. Thus, investigation on the ethanol extract of *G. nutans* was conducted, which led to the isolation of five monoterpene indole alkaloids (**1–5**) and four phenolic glucosides (**6–9**) (Fig. 1). Among the isolated compounds, four compounds (**1–2**, **6–7**) were previously undescribed and others were known. The anti-neuroinflammation activities and cytotoxicities against U87 and HCT116 cell lines were also investigated. Herein, the

[a]*College of Pharmacy, Henan University of Chinese Medicine, Zhengzhou 450046, China*

[b]*The Engineering and Technology Center for Chinese Medicine Development of Henan Province, Zhengzhou 450046, China*

[c]*College of Pharmacy, Chonnam National University, Gwangju 500-757 61186, South Korea. E-mail: imyoungjun@jnu.ac.kr*

[d]*School of Pharmaceutical Sciences, Wenzhou Medical University, Wenzhou 325035, China. E-mail: xianshifree@126.com*

† Electronic supplementary information (ESI) available: The 1D & 2D NMR, and HR-ESI-MS data of compounds **1–9**. See DOI: 10.1039/d1ra05204g

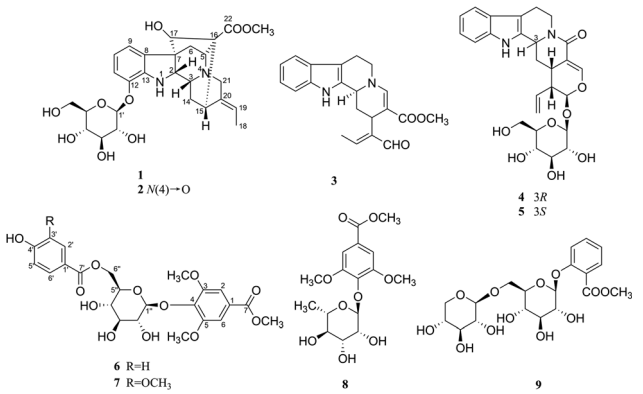

Fig. 1 Structures of compounds 1–9.

isolation, structural elucidation, anti-neuroinflammation activities, and cytotoxicities of these components are discussed.

Results and discussion

Nutanoside A (**1**) was obtained as a white acicular crystal. The molecular formula was determined as $C_{27}H_{34}N_2O_9$ on the basis of the HR-ESI-MS peak at *m*/*z* 531.2359 $[M + H]^+$ ($C_{27}H_{35}N_2O_9$, calcd for 531.2343), corresponding to 12 indices of hydrogen deficiency. The ^{1}H NMR and ^{13}C NMR data (Table 1) displayed signals characteristic of a 1,2,3-trisubstituted phenyl group provided by signals at δ_H 6.84 (1H, d, $J = 7.6$ Hz), 6.75 (1H, t, $J = 7.6$ Hz), 6.56 (1H, d, $J = 7.6$ Hz), and δ_C 143.0 (C-12), 141.7 (C-13), 131.9 (C-8), 119.6 (C-9), 118.2 (C-10), 114.3 (C-11); a methoxy at δ_H 3.53 (3H, s) and δ_C 50.9 (22-OCH_3); a methyl at δ_H 1.52 (3H, d, $J = 6.6$ Hz) and δ_C 12.5 (C-18); a carbonyl group at δ_C 172.7 (C-22); a trisubstituted double bond at δ_H 5.14 (1H, q, $J = 6.6$ Hz) and δ_C 114.2 (C-19), 139.0 (C-20); and a glucosyl group at δ_H 4.67 (1H, d, $J = 7.3$ Hz) and δ_C 101.7 (C-1′), 73.4 (C-2′), 77.1 (C-3′), 69.9 (C-4′), 76.0 (C-5′), 60.9 (C-6′). Comparison of its 1D NMR data with those of quebrachidine[15] indicated that they have a similar monoterpenoid indole alkaloid skeleton, except for the presence of a glucosyl group in compound **1**. The attachment of the glucosyl group to C-12 was confirmed by the correlations from H-1′ (δ_H 4.67) to C-12 (δ_C 143.0) in HMBC spectrum (Fig. 2), and the configuration was confirmed to be β-D by the large coupling constant (7.3 Hz) of the anomeric proton and acid hydrolysis as described in the Experimental section. The NOESY correlations of H-2 with H-5 (Fig. 3) suggested the same β-orientations of H-2 and H-5. The polycyclic rigid framework formed by the connections of C15–C16(C5)–C17–C7 determined the same β-orientations of H-15, H-3 and H-5. The relative configuration at C-17 can be deduced from the observed NOESY correlation signals between H-15 and H-17, which indicated the orientation of H-17 is β. The reciprocal NOESY correlations observed for H-15/H-18 and H-19/H-21 established the geometry configuration of the 19,20-double bond as *E*. Then, theoretical calculations were carried out to determine the absolute configuration of 1. The ECD spectra of (2*R*, 3*R*, 5*S*, 7*R*, 15*S*, 16*R*, 17*S*)-1a and its enantiomer (2*S*, 3*S*, 5*R*, 7*S*, 15*R*, 16*S*, 17*R*)-1b were calculated at B3LYP/6-31+G** level on the base of TDDFT method (Fig. 4).

Table 1 The NMR data of compounds 1–2

	Compound **1**		Compound **2**	
No.	$\delta_H{}^a$ *J* (Hz)	$\delta_C{}^b$	$\delta_H{}^a$ *J* (Hz)	$\delta_C{}^b$
1	5.33 d, 3.2		6.29 s	
2	3.51 d, 4.2	68.9	4.01 br. s	63.4
3	3.34 m	53.8	3.68 br. s	70.9
4				
5	3.22 m	61.0	3.72 d, 3.5	74.7
6	2.40 dd, 10.9, 4.8	36.0	2.31 d, 11.9	31.2
	1.47 d, 10.9		2.24 m	
7		57.7		57.0
8		131.9		129.7
9	6.75 d, 7.6	119.6	6.66 d, 7.7	118.9
10	6.56 t, 7.6	118.2	6.53 t, 7.7	118.6
11	6.84 d, 7.6	114.3	6.77 d, 7.7	112.7
12		143.0		143.4
13		141.7		141.2
14	2.46 dd, 13.8, 4.9	22.1	2.56 dd, 13.2, 4.1	21.8
	1.36 dd, 13.8, 9.9		1.89 t, 11.8	
15	3.35 m	30.0	3.49 d, 4.1	29.0
16		59.9		60.5
17	4.08 d, 6.6	73.2	3.93 s	72.7
18	1.52 d, 6.6, 3H	12.5	1.57 d, 6.2, 3H	12.3
19	5.14 q, 6.6	114.2	5.33 q, 6.2	117.8
20		139.0		131.3
21	3.28 m	54.8	4.22 d, 15.0	69.7
	3.25 m		3.65 m	
22		172.7		170.7
1′	4.67 d, 7.3	101.7	4.73 d, 7.3	100.6
2′	3.23 m	73.4	3.23 m	73.4
3′	3.29 m	77.1	3.32 m	76.8
4′	3.14 m	69.9	3.15 m	70.0
5′	3.26 m	76.0	3.30 m	76.0
6′	3.72 m	60.9	3.71 m	60.9
	3.46 m		3.45 m	
–OCH_3	3.53 s, 3H	50.9	3.60 s, 3H	51.7

[a] Recorded at 500 MHz in DMSO-d_6. [b] Recorded at 125 MHz in DMSO-d_6.

Comparison of the calculated ECD spectra data with that of experimental data of compound **1** indicated the absolute configuration of compound **1** was assigned to be (2*R*, 3*R*, 5*S*, 7*R*, 15*S*, 16*R*, 17*S*).

Nutanoside B (**2**) was obtained as a yellowish oil. It had a molecular formula of $C_{27}H_{34}N_2O_{10}$ by the HR-ESI-MS peak at *m*/*z* 547.2296 $[M + H]^+$ ($C_{27}H_{35}N_2O_{10}$, calcd for 547.2292), which was 16 mass units higher than that of compound **1**. The NMR spectra data (Table 1) were similar to those of **1**, except for the characteristic downfield shifts of the carbon resonances for C-3, C-5, and C-21. Accordingly, the planar structure of compound **2** was identified as the *N*(4)-oxide of compound **1**. The relative configuration was secured by 2D NMR data, including HSQC, HMBC, ^{1}H–^{1}H COSY, and NOESY. The NOESY correlations (Fig. 3) of H-21α with H-2, H-3 and H-5; H-15 with H-17 indicated the same relative configuration at these chiral centers compared with compound **1**. Similarly, the NOESY correlations observed for H-15/H-18 and H-19/H-21 established the geometry configuration of the 19,20-double bond as *E*. In addition, HMBC correlations (Fig. 2) from H-1′ (δ_H 4.73) to C-12 (δ_C 143.4)

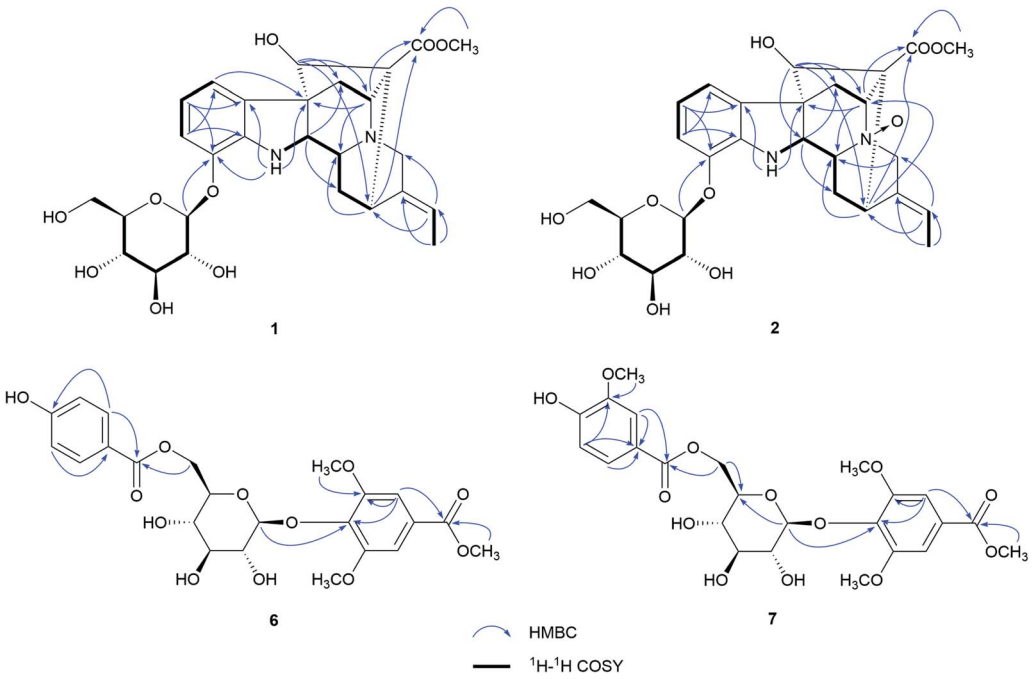

Fig. 2 Key HMBC and $^{1}H-^{1}H$ COSY correlations of **1**, **2**, **6**, and **7**.

assigned the C-12 attachment of the glucosyl moiety, and the coupling constants (7.3 Hz) of anomeric protons and acid hydrolysis established the sugar units as β-D-glucose. The absolute configuration of **2** was established as (2*R*, 3*R*, 5*S*, 7*R*, 15*S*, 16*R*, 17*S*), which was same as **1**, according to their highly similarity on ECD spectrum (Fig. 4). Generally, the glucosyl moiety of monoterpene indole alkaloids are located at monoterpene moiety and occasionally at C-10 or C-11 of the indole skeleton. Compounds **1** and **2** are two rare monoterpene indole alkaloids with the glucosyl moiety located at C-12. Moreover, compounds **1** and **2** represent the first two examples of enantiomer of ajmaline type monoterpene indole alkaloids.

Nutanester A (**6**) was obtained as a yellowish amorphous powder. The molecular formula of **6** was determined as $C_{23}H_{26}O_{12}$ on the basis of the quasi-molecular ion peak at *m*/*z* 517.1334 $[M + Na]^{+}$ ($C_{23}H_{26}O_{12}Na$, calcd for 517.1322) in its HR-ESI-MS spectrum. The ^{1}H NMR and ^{13}C NMR spectrum (Table 2) showed the presence of a 1,3,4,5-tetrasubstituted benzene ring by two magnetically equivalent aromatic proton signals at [δ_H 7.14 (2H, s) and δ_C 124.7 (C-1), 106.8 (C-2, 6), 152.6 (C-3, 5), 137.9 (C-4)], with two magnetically equivalent methoxy by signals at δ_H 3.73 (6H, s) and δ_C 56.2; a 1,4-disubstituted benzene ring at [δ_H 7.55 (2H, d, J = 8.5 Hz), 6.76 (2H, d, J = 8.5 Hz); δ_C 120.2 (C-1′), 131.3 (C-2′, 6′), 115.1 (C-3′, 5′), 162.0 (C-4′)]; a glucosyl group at [δ_H 5.10 (1H, d, J = 6.5 Hz, H-1″); δ_C 101.6 (C-1″), 73.9 (C-2″), 76.5 (C-3″), 70.4 (C-4″), 74.1 (C-5″), 63.5 (C-6″)]; two carbonyl groups at δ_C 165.8 (C-7) and 165.2 (C-7′); and a methoxy at δ_H 3.85 (3H, s) and δ_C 52.2. The connection of the glucose unit at C-4 was confirmed by the HMBC correlation from H-1″ to C-4 (Fig. 2). The *p*-hydroxy benzoyl was shown to be involved in an ester linkage at the C-6″ position by HMBC correlations observed from H-6″ to C-7′. Then, the large coupling constants (6.5 Hz) of anomeric protons, acid hydrolysis and alkaline methanolysis established the sugar units as β-D-glucose. Accordingly, compound **6** was identified as 4-[6-*O*-(*p*-hydroxy

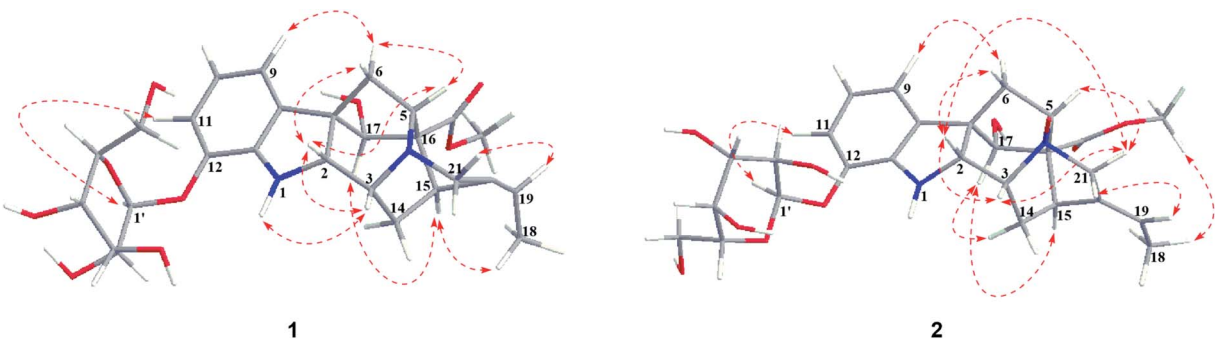

Fig. 3 Key NOESY correlations of **1**–**2**.

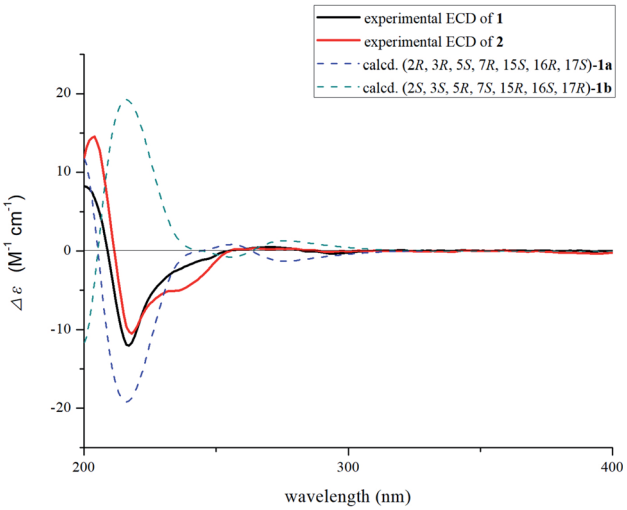

Fig. 4 Calculated ECD spectrum of compound 1 and experimental ECD curves of 1–2.

benzoyl)-β-D-glucopyranoside]-3,5-dimethoxy methyl benzoate, named as nutanester A.

Nutanester B (7) was obtained as a yellowish amorphous powder. The HR-ESI-MS spectrum exhibited a quasi-molecular ion peak at *m/z* 547.1429 $[M + Na]^+$ ($C_{24}H_{28}O_{13}Na$, calcd for 547.1428), allowing the molecular formula of 7 to be assigned as $C_{24}H_{28}O_{13}$, which was 30 mass units higher than that of compound **6**. The ^1H NMR and ^{13}C NMR spectra data (Table 2) were similar to those of **6**, except for the presence of an additional methoxy at [δ_H 3.71 (3H, s); δ_C 55.5]. Meanwhile, the aromatic proton signals for 1,4-disubstituted benzene ring in compound **6** were substituted by a set of ABX coupling proton signals at [δ_H 7.22 (1H, br. s), 6.71 (1H, d, J = 8.1 Hz), and 7.17 (1H, br. d, J = 8.1 Hz)] in compound 7. Thus, compound 7 was identified as the 3′-methoxy substituted analogue of compound **6**, which was further confirmed by 2D NMR spectrum (Fig. 2).

Table 2 The NMR data of compounds 6–7

	Compound 6		Compound 7	
No.	$\delta_H{}^a$ J (Hz)	$\delta_C{}^b$	$\delta_H{}^a$ J (Hz)	$\delta_C{}^b$
1		124.7		124.7
2	7.14 s	106.8	7.13 s	106.8
3		152.6		152.5
4		137.9		138.0
5		152.6		152.5
6	7.14 s	106.8	7.13 s	106.8
7		165.8		165.7
1′		120.2		119.6
2′	7.55 d, 8.5	131.3	7.22 br. s	112.4
3′	6.76 d, 8.5	115.1		147.5
4′		162.0		142.3
5′	6.76 d, 8.5	115.1	6.71 d, 8.1	115.1
6′	7.55 d, 8.5	131.3	7.17 br. d, 8.1	123.5
7′		165.2		165.4
1″	5.10 d, 6.5	101.6	5.11 d, 6.0	101.7
2″	3.27 m	73.9	3.28 m	74.3
3″	3.26 m	76.5	3.27 m	76.5
4″	3.22 m	70.4	3.21 m	70.5
5″	3.38 m	74.1	3.40 m	74.1
6″	4.43 d, 12.1	63.5	4.43 m	63.6
	4.09 dd, 12.1, 7.3		4.10 m	
3,5-OCH_3	3.73 s, 6H	56.2	3.73 s, 6H	56.2
7-OCH_3	3.85 s, 3H	52.2	3.84 s, 3H	52.2
3′-OCH_3			3.71 s, 3H	55.5

[a] Recorded at 500 MHz in DMSO-d_6. [b] Recorded at 125 MHz in DMSO-d_6.

The five known compounds, isovallesiachotamine (**3**),[16] vincosamide (**4**),[17] strictosamide (**5**),[17] methyl syringate 4-*O*-α-L-rhamnoside (**8**),[18] methyl salicylate 2-*O*-β-D-xylosyl (1→6) β-D-glucopyranoside (**9**),[19] were identified by analysis of physicochemical properties and comparison of spectral data with those reported in literatures.

Biological activities

The anti-inflammatory activities of the isolated compounds **1–8** were assayed in BV2 microglial cells by monitoring LPS-induced NO production. Beforehand, cell viabilities of compounds **1–8** on BV2 microglial cells were tested by MTT assay in order to avoid the possible effect of reduced viability on NO release. Results (Fig. 5) showed that compounds **3**, **4**, **8** exhibited cytotoxicity at 10

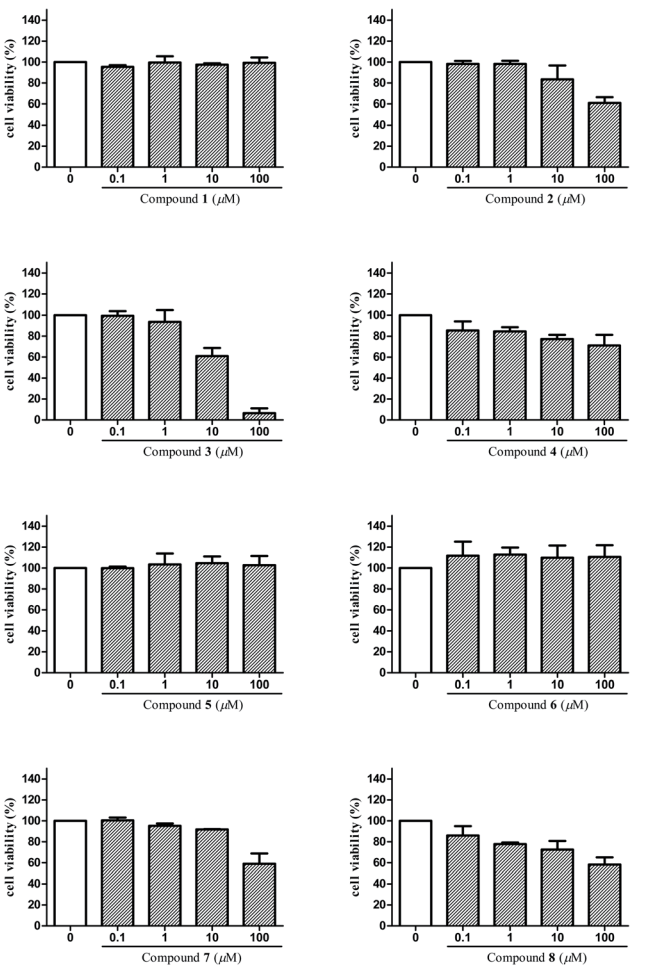

Fig. 5 Cell viability assay of compounds 1–8 in BV2 microglial cells.

Table 3 Inhibitory effects of compounds **1–8** on NO production in LPS-activated microglia cells (mean ± SD)

Compounds	IC_{50} (μM)	Compounds	IC_{50} (μM)
1	74.43 ± 1.34	**5**	15.18 ± 0.81
2	47.30 ± 0.69	**6**	8.78 ± 1.57
3	2.29 ± 0.08	**7**	>100
4	6.36 ± 0.72	**8**	14.41 ± 0.03

μM, and compounds **2**, **7** were toxic to the cells at 100 μM, which may affect their inhibitory effect on LPS-induced NO release. That is to say, such effect of these compounds may mainly due to cell death and not to their inhibitory effect on LPS-induced NO release. Taking this into consideration, concentrations that did not affect the cell viability were selected to test for anti-inflammatory activities of compounds **1–8** in BV2 microglial cells. Among them, 1 μM was the maximum test concentration for compounds **3**, **4**, **8** and 10 μM for compounds **1–2**, **5–7**. As shown in Table 3, compounds **3**, **4** and **6** displayed significant inhibitory effects on NO production in over-activated BV2 microglial cells, with the IC_{50} values of 2.29, 6.36, and 8.78 μM, respectively. In addition, compounds **2**, **5** and **8** also showed moderate inhibitory effects with IC_{50} values ranging from 14.41 to 47.30 μM.

Then, quantitative real-time PCR (qRT-PCR) was also used to further investigate the anti-neuroinflammatory activities of compounds **1–8**. The results (Fig. 6) revealed that compounds **1**, **7** (0.1, 1 and 10 μM), and compound **5** (10 μM) could significantly inhibit the mRNA expression of inflammatory factors TNF-α induced by LPS in BV2 microglial cells. Compounds **5** (1 and 10 μM) and **7** (10 μM) could also greatly inhibit the mRNA expression of inflammatory factors IL-6. In addition, compounds **1**, **3**, **6** and **8** also exhibited a moderate inhibitory effect on the inflammatory factors TNF-α or IL-6 at 0.3–10 μM.

Considering the anti-neuroinflammatory activities and structural characteristics of the isolated compounds, a brief structure–activity relationship (SAR) could be concluded as follows: by comparing compound **4** with **5**, we found that the *3R* configuration could cause an increase of NO inhibitory activity but attenuated the inhibitory effect on inflammatory factors TNF-α and IL-6 in over-activated BV2 microglial cells. A similar situation occurred between compounds **6** and **7**, the presence of 3′-OCH_3 significantly reduced the NO inhibitory activity, while greatly enhanced the inhibitory activities on inflammatory factors TNF-α and IL-6. Moreover, the presence of coordination bond at N-4 in compound **2** (compared with **1**) could weaken the inhibitory effect on inflammatory factors TNF-α and IL-6 in BV2 microglial cells.

Furthermore, considering the effect of some compounds on the survival rate of microglia cells, the cytotoxic activities on two human cancer cell lines (U87 and HCT116) of compounds **3**, **4** and **8** were investigated by MTT method. As shown in Table 4, compound **3** exhibited stronger cytotoxic activities against U87 and HCT116 cell lines than taxol, which was used as the positive control, with IC_{50} values of 10.58 and 14.60 μM, respectively. Compound **4** showed selective inhibitory effect on HCT116 cells with IC_{50} values of 49.21 μM.

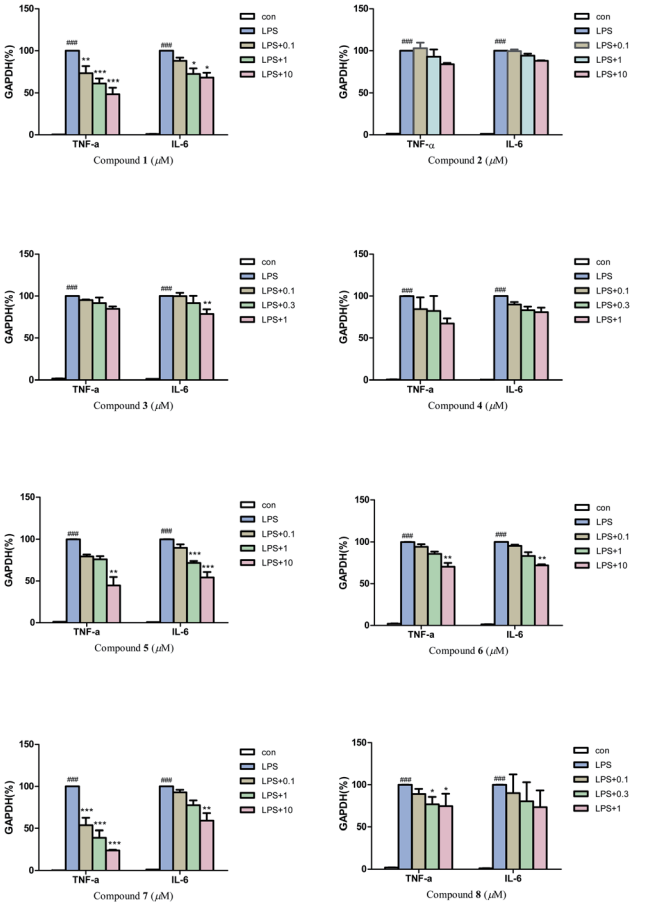

Fig. 6 Effect of compounds **1–8** on LPS-induced mRNA expressions of TNF-α, and IL-6 in BV-2 microglial cells. Each bar represents the means ± SD of three independent experiments. Significance: $^{*}P < 0.05$, $^{**}p < 0.01$, $^{***}p < 0.001$, compared to LPS group; $^{\#\#\#}P < 0.001$, compared to control group.

Table 4 Cytotoxicity data of isolated compounds **3**, **4** and **8**[b]

Compounds	IC_{50} (μM)	
	U87[a]	HCT116[a]
3	10.58 ± 0.23	14.60 ± 0.17
4	>100	49.21 ± 0.03
8	>100	>100
Taxol[c]	16.30 ± 0.06	23.57 ± 0.11

[a] U87, human glioma cell line; HCT116, human colon cancer cell line. [b] Data are expressed as the mean ± SD of three parallel measurements. [c] Positive control.

Experimental method

General experimental procedures

CD spectrum was tested using Chirascanq CD spectrometer (Applied Photophysics) at room temperature. Optical rotation was analyzed using the APIV (Rudolph Research Analytical). NMR spectra were performed on Bruker Avance III 500 MHz spectrometer (Bruker, Karlsruhe, Germany) using TMS as

a standard (500 MHz for ^{1}H NMR and 125 MHz for ^{13}C NMR). Bruker maXis HD mass spectrometer was used to collect HR ESI-TOF MS data in *m*/*z* (rel.%). MPLC was performed on Agela ODS flash column (C-18, 120 g, 40–60 μm, Tianjin, China), and the FL-H050G MPLC system (Tianjin, China). HPLC separation was carried out on a semi-preparative YMC-pack ODS-A column (250 × 10 mm, YMC-pack, Kyoto, Japan) equipped with Saipuruisi LC-52 instrument with a UV200 detector (Beijing, China). Silica gel GF254 for TLC and silica gel (200–300 mesh) for column chromatography were obtained from Qingdao Haiyang Chemical Co., Ltd. (Qingdao, China). D-Glucose and L-glucose (SigmaAldrich, St. Louis, MO, USA) were used to determine the absolute configuration of sugar moiety. Sephadex LH-20 for column chromatography was obtained from Pharmacia (Piscataway, NJ, USA).

Plant material

The whole plant of *Gardneria nutans* Siebold & Zuccarini was collected from Guizhou province, China, in October, 2018, and identified by Prof. Cheng-Ming Dong (Henan University of Chinese Medicine). A voucher specimen (no. 201810) was deposited in the Research Department of Natural Product Chemistry, School of Pharmacy, Henan University of Chinese Medicine.

Extraction and isolation

The dried whole plant of *G. nutans* (17.5 kg) were extracted with 95% ethanol under reflux for three times (2 h/time). After concentration and combination, the crude extract was dispersed in 0.5% HCl and extracted with isopyknic EtOAc for three times. The acidic water layer was basified with 10% ammonia solution to pH 9–10 and extracted with EtOAc to give an alkaloidal extract (17 g). The alkaloidal extract was subjected to MPLC on ODS column, eluting gradually with MeOH–H_2O (20 : 80, 40 : 60, 60 : 40, 80 : 20, and 100 : 0, v/v) to afford five fractions Fr. A–E. Fr. B was applied to a silica gel column and eluted with a CH_2Cl_2–MeOH gradient (from 100 : 0 to 0 : 100) to afford 11 fractions Fr. B1–B11. Fr. B9 was further purified by semi-preparative HPLC eluted with 32% MeOH–H_2O to yield compound **1** (20 mg, t_R = 64 min). Fr. B10 was chromatographed over pre-HPLC (MeOH–H_2O, 22 : 78, v/v) to yield compound **2** (12.5 mg, t_R = 32 min). Fr. B4 was further purified by pre-HPLC (MeOH–H_2O, 40 : 60, v/v) to afford compounds **6** (2.1 mg, t_R = 57 min), **7** (1.5 mg, t_R = 50 min), and **8** (4.6 mg, t_R = 38 min). Fr. B7 was applied to Sephadex LH-20 with MeOH eluent to obtain ten fractions Fr. B7-1–B7-10, and then compound **9** (13.4 mg, t_R = 21 min) was obtained from Fr. B7-4 by pre-HPLC (MeOH–H_2O, 35 : 65, v/v). Fr. C was subjected to Sephadex LH-20 (MeOH) to give four fractions Fr. C1–C4. Fr. C3 was chromatographed on a silica gel column eluting with CH_2Cl_2–MeOH (20 : 1, 13 : 1, 1 : 0) to give 16 subfractions Fr. C3-1–C3-16. Compound **4** (3.6 mg, t_R = 42 min) was obtained from Fr. C3-5 by pre-HPLC (48% MeOH), and compound **5** (2.8 mg, t_R = 23 min) was yielded from Fr. C3-12 by pre-HPLC (57% MeOH). Compound **3** (41 mg) was purified by Sephadex LH-20 (MeOH) and recrystallization from Fr. D.

Nutanoside A (**1**), white acicular crystal; $[\alpha]_D^{25}$-68.28 (*c* 0.07, MeOH); IR ν_{max} 3369, 1645, 1463, 1297, 1249, 1207, 1017 cm^{-1}; ^{1}H NMR (500 MHz, DMSO-d_6) and ^{13}C NMR (125 MHz, DMSO-d_6) see Table 1; HR-ESI-MS *m*/*z* 531.2359 [M + H]$^+$ (calcd for $C_{27}H_{35}N_2O_9$, 531.2343).

Nutanoside B (**2**), yellowish oil; $[\alpha]_D^{25}$-13.10 (*c* 0.07, MeOH); IR ν_{max} 3314, 2923, 1731, 1593, 1482, 1458, 1230, 1244, 1206, 1175, 1076, 1042, 879, 742 cm^{-1}; ^{1}H NMR (500 MHz, DMSO-d_6) and ^{13}C NMR (125 MHz, DMSO-d_6) see Table 1; HR-ESI-MS *m*/*z* 547.2296 [M + H]$^+$ (calcd for $C_{27}H_{35}N_2O_{10}$, 547.2292).

Nutanester A (**6**), yellowish amorphous powder; IR ν_{max} 3424, 1698, 1640, 1608, 1502, 1462, 1341, 1277, 1126, 1066, 1018, 768, 699 cm^{-1}; ^{1}H NMR (500 MHz, DMSO-d_6) and ^{13}C NMR (125 MHz, DMSO-d_6) see Table 2; HR-ESI-MS *m*/*z* 517.1334 [M + Na]$^+$ (calcd for $C_{23}H_{26}O_{12}Na$, 517.1322).

Nutanester B (**7**), yellowish amorphous powder; IR ν_{max} 3486, 2920, 1649, 1258, 775, 725, 701 cm^{-1}; ^{1}H NMR (500 MHz, DMSO-d_6) and ^{13}C NMR (125 MHz, DMSO-d_6) see Table 2; HR-ESI-MS *m*/*z* 547.1429 [M + Na]$^+$ (calcd for $C_{24}H_{28}O_{13}Na$, 547.1428).

Absolute configurations determination of sugar moieties

Compounds **1–2** (each 1.0 mg) were separately treated with 2 M HCl (2 mL) for 3 h at 85 °C. Each reaction product was dissolved in H_2O after evaporation and then extracted with $CHCl_3$ for three times. After being concentrated to dryness, the aqueous layer was subjected to HPLC on a chiral-phase CHIRALPAK AD-H column (250 × 4.6 mm) eluting with *n*-hexane: EtOH : TFA (750 : 250 : 0.25, v/v/v, 0.5 mL min^{-1}), and equipped with an evaporative light scattering detector (ELSD). D-Glucose was detected in the acid hydrolysates of compounds **1–2** according to their same retention times with those of known D-glucose (t_R = 18.3 min) in the same condition.

Compounds **6–7** (each 1.0 mg) were treated with 6% NaOMe in MeOH (2 mL) at room temperature for 2 h. The reaction mixture was dissolved in H_2O after evaporation and then extracted with $CHCl_3$ for three times. The aqueous layer was dried and then D-glucose was determined by using acid hydrolysis method described above.

Anti-inflammatory assay in BV2 cells

Cell viability was detected by MTT method. Cells were seeded in 96-well plates (3 × 10^5 cells per mL) and incubated for 24 h. After treatment with tested compounds for 24 h, cells were incubated with MTT (0.25 mg mL^{-1}) for 4 h at 37 °C. The culture medium was removed, and then the crystals were dissolved in DMSO. The cell viability rate was measured by optical densities at 570 nm with a microplate reader.

The nitrite concentration was measured in the supernatant of cells by the Griess reagent system according to protocol. Cells were seeded into 96-well plates and treated with tested compounds in presence of LPS (100 ng mL^{-1}) for 24 h. 50 μL of culture supernatant fluids were mixed with 50 μL Griess reagent at room temperature, and then the absorbance at 540 nm was determined after 15 min.

Quantitative real-time PCR

BV-2 microglial cells were seeded in 96-well plates (4×10^5 cells per mL) and incubated for 24 h. After treatment with tested compounds for 1 h, cells were incubated with LPS (100 ng mL^{-1}) for 24 h. Total RNA was extracted with Trizol (Invitrogen) according to the manufacturer's protocol, and qRT-PCR assays were performed with the CFX Connect™ real-time PCR detection system (Bio-Rad) using total RNA and the GoTaq one-step real-time PCR kit with SYBR green.

Cytotoxicity assay

A MTT assay was used to determine the cytotoxicity of each compound against two cultured human cancer cell lines. The cell lines used were U87 (human glioma cell line) and HCT116 (human colon cancer cell line). In brief, cells suspensions were plated in 96-well microtiter plates (2.5×10^4 cells per mL) and incubated for 24 h at 37 °C under 5% CO_2. After treatment with tested compounds for 72 h, cells were incubated with MTT (50 μL, 0.4%) for 4 h at 37 °C. Then, the MTT was removed from the wells and the formazan crystals were dissolved in DMSO (200 μL) for 10 min with shaking. The plate was read immediately on a microtiter plate reader at a wavelength of 570 nm to record the optical density. The IC_{50} value was defined as the concentration of the control in the MTT assay. Taxol was used as a positive control.

ECD computation method

Conformational search of compound **1** was carried out by Spartan software using the MMFF94S force field. Then, the structural optimization of target conformations was performed by DFT theory at the B3LYP/6-31G* level. TDDFT ECD calculations for these optimized conformers were carried out at the B3LYP/6-31+G* level with a CPCM model in MeOH solvent.[20]

Conclusions

In this research, a phytochemical investigation on the ethanol extract of *G. nutans* was carried out and led to the isolation of two new monoterpene indole alkaloid glycosides nutanoside A–B (**1–2**), two new phenolic glycoside esters nutanester A–B (**6–7**) and five known compounds (**3–5**, **8–9**). Compounds **1** and **2** are two rare monoterpene indole alkaloids with the glucosyl moiety located at C-12. Moreover, compounds **1** and **2** represent the first two examples of enantiomer of ajmaline type monoterpene indole alkaloids. The results of anti-neuroinflammatory activities showed that compounds **3**, **4** and **6** displayed significant inhibitory effects on NO production in over-activated BV2 microglial cells, with the IC_{50} values of 2.29, 6.36, and 8.78 μM, respectively, and compounds **1**, **5**, **7** could significantly inhibit the mRNA expression of inflammatory factors TNF-α and IL-6 induced by LPS in BV2 microglial cells at the effective concentration, which provide evidence for compounds **1**, **3–7** to be used as leading compounds for medicine design for neurodegenerative diseases. In addition, compound **3** exhibited stronger cytotoxicities against U87 and HCT116 cell lines than taxol, which indicated that compound **3** could be potential antitumor drug candidates.

Conflicts of interest

There are no conflicts to declare.

Acknowledgements

This research project was financially supported by the 2018 doctoral research start-up foundation of Henan University of Chinese Medicine (BSJJ2018-02), and innovation training program for college students of Henan University of Chinese Medicine (No. 202110471034).

Notes and references

1 F. D. Zhu, Y. J. Hu, L. Yu, X. G. Zhou, J. M. Wu, Y. Tang, D. L. Qin, Q. Z. Fan and A. G. Wu, *Front. Pharmacol.*, 2021, **12**, 683935.
2 S. Koppula, R. Alluri and S. R. Kopalli, *EXCLI J.*, 2021, **20**, 835–850.
3 M. Guo, Y. Hao, Y. Feng, H. Li, Y. Mao, Q. Dong and M. Cui, *Front. Mol. Neurosci.*, 2021, **14**, 630808.
4 M. Colonna and O. Butovsky, *Annu. Rev. Immunol.*, 2017, **35**, 441–468.
5 D. V. Hansen, J. E. Hanson and M. Sheng, *J. Cell Biol.*, 2018, **217**, 459–472.
6 Z. Fan, D. J. Brooks, A. Okello and P. Edison, *Brain*, 2017, **140**, 792–803.
7 J. D. Alibhai, A. B. Diack and J. C. Manson, *FASEB J.*, 2018, **32**, 5766–5777.
8 W. X. Yang, Y. F. Chen, J. Yang, T. Huang, L. L. Wu, N. Xiao and Y. H. Zhang, *Fitoterapia*, 2018, **124**, 8–11.
9 J. H. Jiang, Y. M. Zhang, Y. Zhang, G. M. Yang and Y. G. Chen, *Yunnan Chem. Technol.*, 2012, **39**, 32–35.
10 X. H. Zhong, L. Xiao, Q. Wang, B. J. Zhang, M. F. Bao, H. X. Cai and L. Peng, *Phytochem. Lett.*, 2014, **10**, 55–59.
11 T. Feng, X. N. Li, B. H. Zhang, Y. Li, X. H. Cai, Y. P. Liu and X. D. Luo, *Bioorg. Med. Chem. Lett.*, 2013, **23**, 5563–5565.
12 W. X. Yang, T. Huang, J. X. Zhang, J. H. Liu, X. J. Hao and Y. H. Zhang, *Chin. Pharm. J.*, 2016, **51**, 1113–1115.
13 G. H. Xie, L. Ma, Z. P. Zhang and L. H. Hu, *Chin. J. Nat. Med.*, 2007, **5**, 255–258.
14 M. Harada and Y. Ozaki, *Chem. Pharm. Bull.*, 1978, **26**, 48–52.
15 M. R. Yagudaev, *Chem. Nat. Compd.*, 1982, **18**, 693–696.
16 F. Bahadori, G. Topçu, M. Boğa, A. Türkekul, U. Kolak and M. Kartal, *Nat. Prod. Commun.*, 2012, **7**, 731–734.
17 Z. Z. Zhang, H. N. ElSohly, M. R. Jacob, D. S. Pasco, L. A. Walker and A. M. Clark, *J. Nat. Prod.*, 2001, **64**, 1001–1005.
18 Y. L. Wang, Y. J. Li, A. M. Wang, X. He, S. G. Liao and Y. Y. Lan, *J. Asian Nat. Prod. Res.*, 2010, **12**, 765–769.
19 J. Li, F. Li, Y. Y. Lu, Y. J. Zhang and X. S. Huang, *Guangxi Sci.*, 2006, **13**, 217–218, 225.
20 Y. Y. Si, M. X. Tang, S. Lin, G. Chen, H. M. Hua, J. Bai, Y. B. Wang, H. F. Wang and Y. H. Pei, *J. Asian Nat. Prod. Res.*, 2019, **21**, 528–534.